Multi-Terminal Attitude Manipulator Testbed

1st René Rüddenklau
Institute of Communications and Navigation
Optical Satellite Links
German Aerospace Center (DLR)
Weßling, Germany
https://orcid.org/0000-0003-2876-8591

2nd Christopher Schmidt
Institute of Communications and Navigation
Optical Satellite Links
German Aerospace Center (DLR)
Weßling, Germany
https://orcid.org/0009-0008-0485-3541

***Abstract*—Upcoming free-space optical communication missions will require simultaneous, multi-link operation using several optical terminals on small satellite platforms. Achieving submilliradian pointing stability under these conditions demands coordinated control of actuators with diverse bandwidths, ranges, and accuracy. This paper presents a multi-terminal attitude manipulator testbed, developed for hardware-in-the-loop validation of such systems. The setup combines precise attitude emulation, fine and coarse pointing assemblies, and real-time optical tracking emulation to evaluate sensor calibration, control allocation, and feed-forward compensation strategies. Experimental results demonstrate improved attitude knowledge propagation through online bias estimation, improved risk mitigation through micro-vibration testing, and stable offloading between fine and coarse actuators. The testbed provides a flexible, high-fidelity environment to validate distributed control and coordination concepts, bridging the gap between simulation and in-orbit testing for next-generation optical communication networks.**

***Index Terms*—Free-Space Optical Communication, Hardware-in-the-Loop, Attitude Control, Multi-Link Optical Terminals, Over-Actuated Systems.**

I. INTRODUCTION

Future free-space optical communication (FSOC) systems for space applications will not only serve as high-capacity data relays for classical communication, but will also enable precise time transfer, ranging, and quantum key distribution [1], [2]. A recent use case is demonstrated by the company Kepler, which is launching a next-generation optical data relay network in January 2026, featuring ten satellites, each equipped with a minimum of four optical terminals, enabling high-throughput laser links for real-time, low-latency connectivity between space, air, and ground assets [3]. A central challenge in all optical communication scenarios lies in achieving highly accurate and efficient pointing, acquisition and tracking (PAT) functionality. The host satellite's attitude control provides the baseline for overall pointing accuracy, which can be further enhanced by incorporating dedicated actuators within the optical communication subsystem.

Typically, a fine pointing assembly (FPA) enables fine laser beam steering based on optical feedback from a tracking sensor, achieving control bandwidths up to the kilohertz regime. Complementarily, a coarse pointing assembly (CPA) extends the field of regard (FOR), allowing pointing with fewer restrictions on spacecraft orientation. Managing multiple actuators with differing bandwidths and performance constraints requires a carefully designed control allocation strategy to make optimal use of their combined capabilities. This challenge becomes even more significant in multi-link scenarios, where separate but simultaneous pointing objectives must be fulfilled. In such cases, dynamic control allocation [4] provides notable benefits, particularly for FSOC in satellite constellations or CubeSat missions [5]. While CubeSats offer cost-effective access to space, their limited attitude control performance emphasizes the importance of advanced, multi-actuator coordination and test validation under realistic hardware conditions.

This work addresses the need for a dedicated multi-terminal attitude manipulator (MTAM) testbed capable of demonstrating hardware-in-the-loop operation of multiple optical links. Such an experimental platform is essential to verify acquisition and control allocation methods, validate actuator coordination concepts, and assess tracking performance under realistic, coupled system dynamics before on-orbit deployment. In Section II prerequisites as well as specific demands for laser communication terminal (LCT) systems are described. In Section III the specific implementation and initial results of the MTAM testbed are analyzed.

II. MISSION DEMANDS FOR SATELLITE LASER COMMUNICATIONS SYSTEMS

A. Satellite Laser Communication Systems

The number of optical communication terminals deployed in space continues to grow steadily [6], largely driven by the expansion of large satellite constellations [1], [7], [8]. These missions often require multiple optical terminals mounted on a single spacecraft platform to support simultaneous inter-satellite and ground links. Although individual terminal designs vary, most rely on a combination of three key actuator types, described in the following.

The use of FSOC aboard mobile platforms such as unmanned aerial vehicles, high-altitude platforms, aircraft, or satellites is particularly advantageous because these platforms can provide unobstructed optical paths over long distances. As shown in Figure 1, this work focuses on satellite-based configurations, which serve as representative effectors. The figure illustrates the typical components of a satellite LCT.

Funded by the Bavarian Transformation and Research Foundation (Bayrische Transformations- und Forschungsstiftung).

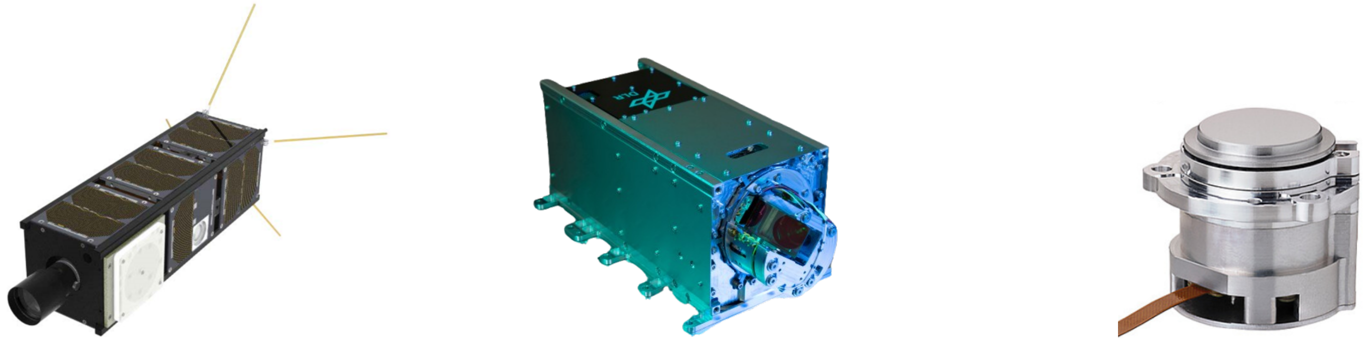

(a) (b) (c)

Fig. 1: Representative illustrations of FSOC subsystems with (a) an integrated 3U CubeSat, (b) a hemispherical CPA designed in a gimbaled prism configuration, and (c) a commercial hybrid reluctance actuator (HRA) fine steering mirror (FSM) [9].

Including the spacecraft and its attitude determination and control system (ADCS) in the analysis is critical, as the satellite's body pointing cannot be decoupled from the pointing of the LCT. A single platform can host several LCTs to establish both inter-satellite and ground connections. Commonly, an LCT integrates a CPA to extend its pointing range and an FPA to maintain fine alignment and compensate for high-frequency disturbances [10]. Depending on the mission, additional actuators may be integrated—for instance, for fiber coupling or point-ahead angle adjustment. Multiple attitude references, such as inertial measurement units, horizon sensors, sun sensors, and magnetometers, complement the dedicated tracking sensors of each terminal, which may employ quadrant photodiodes [11], position-sensitive devices [12], or focal plane arrays [13]. Dual-sensor configurations with differing field of view (FOV) are also common to facilitate rapid acquisition and precise tracking [14].

Control allocation is therefore proposed to consider the heterogeneous sensor inputs and actuator characteristics of over-actuated FSOC systems. For constellation missions in particular, coordinated multi-terminal control is essential, motivating the need for an experimental platform to test such distributed, high-precision pointing strategies under realistic hardware conditions.

B. Master Attitude Controller

A concept to address these challenges is being developed within the optical space infrared downlink system (OSIRIS) mission framework. The proposed master attitude controller (MAC) unit [15] functions as a centralized control and coordination element for multi-terminal systems. This section outlines the general principles and hardware components of the concept.

Requirements for the MAC derive from state-of-the-art missions and commercial solutions. During acquisition, the ADCS provides the most accurate attitude information relative to the optical link target, crucial for improving link acquisition probability and reducing mean acquisition time [16]. However, due to limited update rates, it cannot compensate for high-speed pointing errors, highlighting the need for self-contained attitude sensing within the LCT that can propagate the highly accurate ADCS attitude estimation between updates and feed-forward it to the fine pointing assembly to pre-distort the scan pattern [10].

During optical tracking, the ADCS could benefit from enhanced pointing data from the LCT, yet most CubeSat buses do not natively support such feedback integration. Implementing this interface would typically require custom engineering effort. The MAC offers a higher-level integration alternative by utilizing existing pointing offset interfaces on standard satellite buses, allowing the LCT to provide high-rate reference updates while preserving platform safety constraints. This setup mitigates issues such as star tracker dropouts during fast rotations and allows continuous link stability [11]. The MAC thus provides a modular and scalable foundation for multi-link operations across heterogeneous platforms.

C. Multi-Link Scenario

In over-actuated systems, additional degrees of freedom can be leveraged to meet secondary objectives while maintaining primary pointing constraints. Figure 2 illustrates key constraints and optimization goals for a typical space laser communication system. Primary constraints include actuator range limits, environmental conditions, and link stability requirements, while optimization goals may target energy efficiency, actuator health, or future link preparation.

Optimization can further balance power consumption, minimize actuator wear, and reserve dynamic range for future links. In some cases, optimization priorities can shift dynamically. For example, when power levels become critical, solar array pointing may temporarily take precedence over link maintenance [5].

To evaluate actuator performance trade-offs, the currently state-of-the-art derived achievable range-bandwidth product (RBP) Pareto front is shown in Figure 3, illustrating the trade-off between range, bandwidth, and accuracy for representative subsystems. Although these actuators share overlapping performance regions, wide-range devices generally exhibit lower

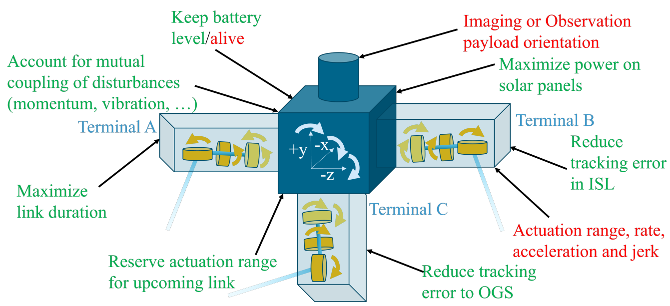

Fig. 2: Examples of control allocation constraints (red) and optimization objectives (green) for a multi-link space laser communication system [5].

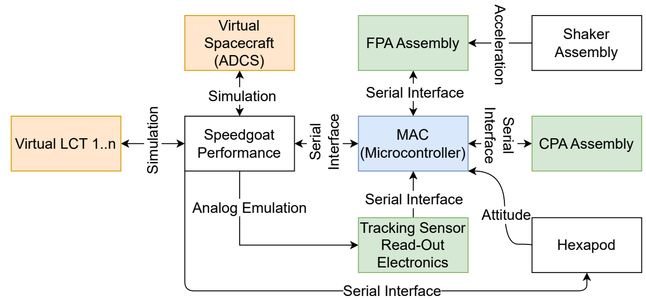

Fig. 4: MTAM testbed setup using test equipment (white) to enable real-time simulation (orange), hardware-in-the-loop (green) and processor-in-the-loop (blue) capabilities.

accuracy and bandwidth, reinforcing the need for hybrid, multi-actuator architectures.

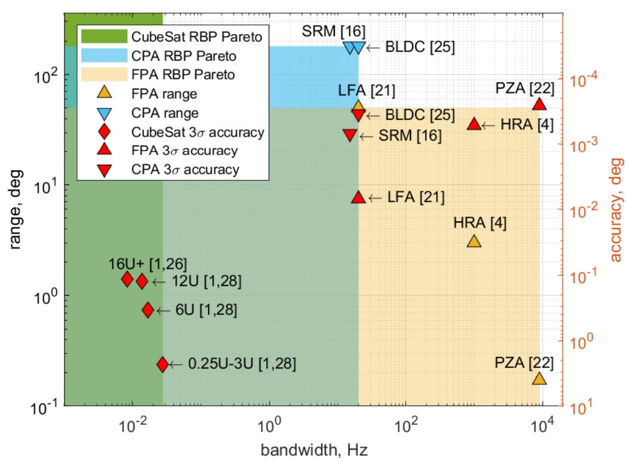

Fig. 3: Actuator Pareto front illustrating the trade-off between range, bandwidth, and precision across actuator types [5].

In this context, a dedicated testbed becomes indispensable to experimentally validate control allocation strategies [5], verify actuator coordination, and explore optimization trade-offs in multi-link configurations. The subsequent section defines representative subsystem analysis and outlines the structure of the proposed hardware-in-the-loop test environment.

III. Implementation of the Testbed

A. Multi-Terminal Attitude Manipulator Testbed Design

The proposed MTAM testbed has been developed to emulate realistic space optical link conditions, enabling hardware-in-the-loop validation of control algorithms and multi-link coordination strategies. Figure 4 shows the proposed testbed including the interfaces to connect all involved subsystems.

The central test infrastructure unit is built by a real-time capable processing unit by the company Speedgoat. It allows to run Simulink models while establishing a connection to surrounding hardware through analog and digital interfaces. It therefore simulates the dynamics of the satellite and a variable number n of virtual LCTs. The attitude of the virtual spacecraft is coupled to the input of the tracking sensor read-out electronics—that would be usually connected to a quadrant photo diode (QPD)—and to the hexapod to manipulate the readings of the employed gyroscope sensor accordingly. The emulated tracking sensor inputs are forwarded to the MAC, which will use this input together with the inputs of the virtual LCTs to allocate the control commands. The CPA has its own low-level servo control, which will return the measured position encoder readings. The FPA is likewise locally closed-loop controlled, but has an additional source of disturbance which emulates micro-vibrations on board of the spacecraft through a dedicated shaker setup (see Sec. III-C).

The setup integrates measurement and emulation equipment designed to replicate dynamic characteristics of a satellite-based FSOC system. This is not limited only to laboratory tests but can also be used to demonstrate early prototypes during ground-to-ground link operation [17]. In the following, the different subparts of the proposed testbed are analyzed.

B. Sensor Supported Acquisition

The subsequent analysis will focus on the validation of the sensor calibration and attitude propagation to feed-forward the augmented knowledge to the LCT [10]. To ensure accurate attitude propagation, the micro-electro-mechanical system (MEMS) gyroscope sensors of the LCT must first be calibrated both statically and dynamically to ensure robust sensor readings, also during temperature variations, as depicted in Figure 5, which shows the estimated bias evolution. In the test setup, the terminal is rotated on a precision turntable at multiple angular rates around each axis. The test sequence includes rotations of $15\,\mathrm{deg\,s^{-1}}$, $-10\,\mathrm{deg\,s^{-1}}$, $5\,\mathrm{deg\,s^{-1}}$, $-2.5\,\mathrm{deg\,s^{-1}}$, $1.25\,\mathrm{deg\,s^{-1}}$ and $-10\,\mathrm{deg\,s^{-1}}$, each maintained for approximately $10\,\mathrm{s}$ to $20\,\mathrm{s}$. This variety of motion ensures that the calibration process does not overfit the estimated parameters to a specific dynamic condition as expected in orbit.

As spacecraft experience temperature fluctuations during eclipse transitions, sensor biases can drift over time. To address this, the developed online bias estimation algorithm [10] continuously compensates for thermal effects. A validation

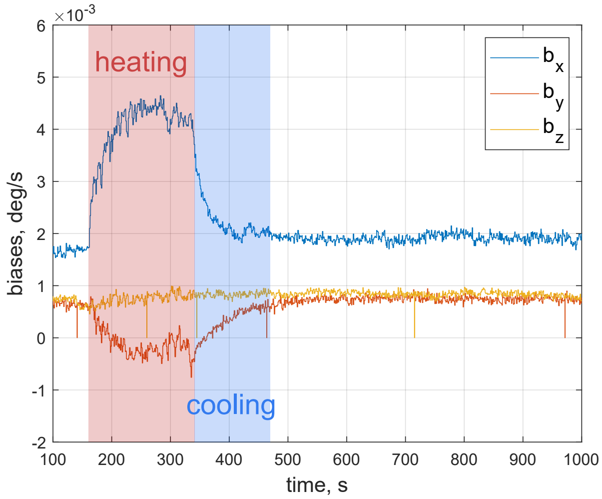

(a)

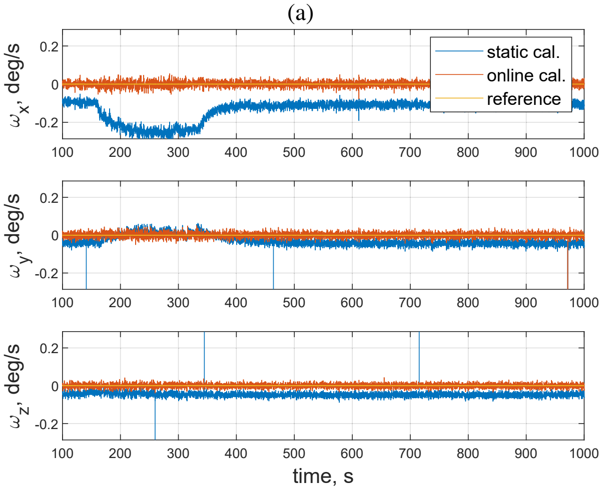

(b)

Fig. 5: (a) Online bias estimation during temperature changes and (b) comparison between online and static calibration results of the gyroscope sensor [10].

experiment was performed by heating the gyroscope sensor to approximately $50\,°\mathrm{C}$ using a hot air source. During the heating and cooling phases, noticeable bias shifts occur (Fig. 5a), yet the online-calibrated rates remain close to the reference (Fig. 5b), confirming the robustness of the real-time temperature compensation approach.

C. Actuator Based Tracking

The tracking phase can also be covered by the MTAM, which analysis focuses on actuator-level behavior in closed-loop operation (see Fig. 6). The expected vibration level of the satellite is injected by the vibration setup to emulate realistic spacecraft environment during reaction wheel operation. The experimental setup integrates a fine pointer with read-out electronics and an electronic driver, operated under hardware-in-the-loop control by the Simulink driven Speedgoat system. Results show that the testbed can be used to predict in-orbit performance of the employed actuator under vibrations. This is not only helpful to tune the desired control algorithm, but also to test other parts of the signal chain, like the electronic driver or the read-out electronics. It can be further used to optimize damping strategies based on the measured results.

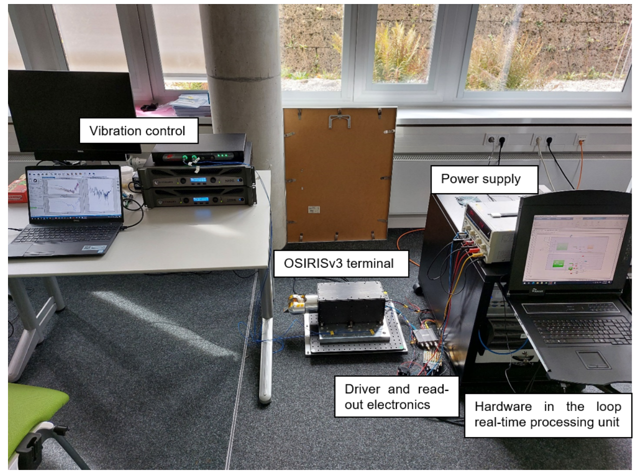

(a)

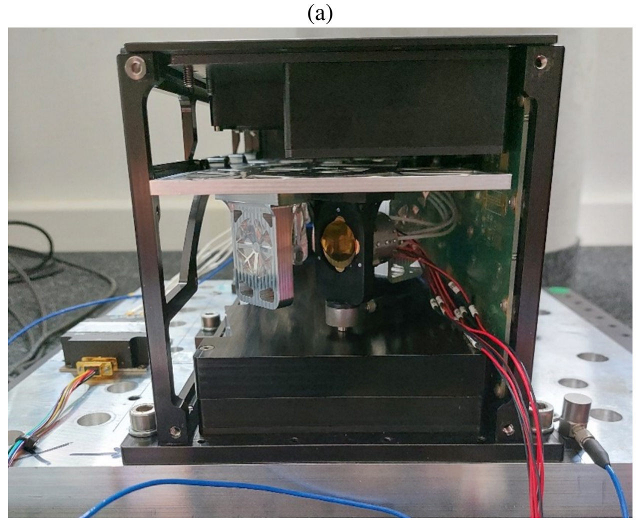

(b)

Fig. 6: (a) Vibration testing setup with real-time hardware-in-the-loop control and measurement capability of (b) the FSM inside the optical terminal.

Figure 7 summarizes the vibration testbed results. The input spectrum, which is defined by the spacecraft, is introduced to the optical terminal at the mounting interface. This spectrum is used as the control command for the vibration shaker. The LCT amplifies the spectrum, resulting in the measured spectrum at the FSM mount (see Figure 6b). The test was performed with the FSM running in closed-loop control with a setpoint of 0 degrees, which corresponds to the initial central position. The remaining error was recorded as time history data over a period of 60 seconds. This data was then transformed into the frequency domain to display any frequency correlation with the provided input spectrum.

The evaluation shows that using a 3σ confidence interval results in an error of $109.2\,\mu\mathrm{rad}$, which exceeds the requirement of 12 µrad (for this specific use case) by an order of magnitude. Therefore, passive countermeasures were installed at the source of the disturbance to reduce the vibration load above 250 Hz. Consequently, the input was reduced, and the modified measured curve was generated. The result obtained is within the requirement, leaving a residual angular jitter of 5.49 µrad. Additionally, a simulation model was compared with the same modified spectrum. The absolute deviation of the RMS value is 0.93 µrad meaning the model underestimates the jitter attributed to neglecting imperfections in the hardware system.

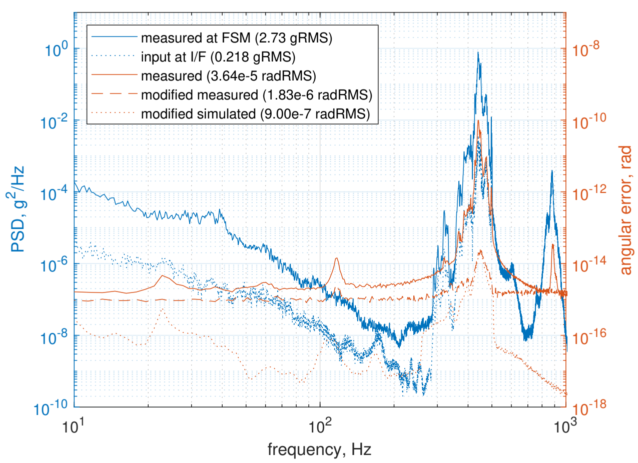

Fig. 7: Summary of the vibration testbed data. In blue, the power-spectral-density defining the controlled input and measured output at the device-under-test. In red, the measured and simulated angular excitation of the FSM in closed-loop operation.

Table I lists the current capabilities of the testbed. This means that, after completing the LCT model and tracking sensor emulation, a fully operational multi-terminal testbed for control allocation is available.

TABLE I: MTAM requirements evaluation

Requirement	**Status**	**Reference**
Gyroscope Calibration	✓	Sec. III-B
Actuator Closed-Loop Control	✓	Sec. III-C
Micro-Vibration	✓	Sec. III-C
MAC (Processor-In-The-Loop)	✓	[15]
Satellite Model	✓	[18]
LCT Model	ongoing	-
Tracking Sensor Emulation	ongoing	-
Multi-Terminal Control Allocation	ongoing	-

Note that parts of the presented results in this work rely on previous work, as indicated. However, this paper demonstrated how to achieve a versatile testbed for upcoming missions based on those insights. The presented results therefore indicate a working MTAM testbed basis that can be used for inter-actuator testing, including external environmental disturbances, before full system integration and therefore paves the way for future multi-terminal scenario performance analysis.

IV. Conclusion

The presented MTAM testbed provides a versatile hardware-in-the-loop platform to evaluate coordinated control strategies for future FSOC missions. It enables the validation of multi-actuator and multi-link control allocation approaches under realistic mechanical, optical, and dynamic conditions. The integration of precise sensor calibration, online bias estimation, and closed-loop tracking demonstrates the testbed's capability to emulate complete LCT behavior with realistic dynamics through hardware-in-the-loop actuation and feedback.

This experimental infrastructure bridges the gap between simulation and in-orbit validation, offering a crucial step toward scalable and reliable optical inter-satellite communication networks. Future work will extend the setup to simultaneously operate multiple optical terminals, enabling end-to-end testing of dedicated control allocation algorithms integrating the ADCS into the loop.

Acknowledgment

The authors would like to thank all involved colleagues from the Optical Satellite Links department for their valuable contributions. Funded by the Bavarian Transformation and Research Foundation (Bayrische Transformations- und Forschungsstiftung).

References

[1] A. U. Chaudhry and H. Yanikomeroglu, "Laser intersatellite links in a starlink constellation: A classification and analysis," *IEEE Vehicular Technology Magazine*, vol. 16, no. 2, pp. 48–56, 2021.

[2] C. Fuchs, D. Laidlaw, F. Moll, J. Poliak, C. Schmidt, and A. Shrestha, "Recent results in optical satellite link research at dlr," in *Free-Space Laser Communications XXXVII*, H. Hemmati and B. S. Robinson, Eds. SPIE, 25.01.2025 - 31.01.2025, p. 2. [Online]. Available: https://www.spiedigitallibrary.org/conference-proceedings-of-spie/13355/3040371/Recent-results-in-optical-satellite-link-research-at-DLR/10.1117/12.3040371.full

[3] Crystalyn Koch, "Kepler announces launch date for first tranche of optical satellites," 17.11.2025. [Online]. Available: https://kepler.space/kepler-announces-launch-date-for-first-tranche-of-optical-satellites/

[4] T. A. Johansen and T. I. Fossen, "Control allocation—a survey," *Automatica*, vol. 49, no. 5, pp. 1087–1103, 2013.

[5] R. Rüddenklau and G. Schitter, "Control allocation for over-actuated satellite laser communication systems," *Acta Astronautica*, vol. 240, pp. 522–529, 2026. [Online]. Available: https://www.sciencedirect.com/science/article/pii/S0094576525008914

[6] S. V. Weston, C. D. Burkhard, J. M. Stupl, R. L. Ticknor, B. D. Yost, R. A. Austin, P. Galchenko, L. K. Newman, and L. Santos Soto, "State-of-the-art small spacecraft technology," National Aeronautics and Space Administration, Ames Research Center, Moffett Field, CA 94035-1000, NASA/TP NASA/TP—20250000142, February 2025. [Online]. Available: https://www.nasa.gov/smallsat-institute/sst-soa/

[7] J. C. McDowell, "The low earth orbit satellite population and impacts of the spacex starlink constellation," *The Astrophysical Journal Letters*, vol. 892, no. 2, p. L36, 2020.

[8] B. Koosha, P. Madani, and M. D. Ardakani, "Comprehensive analysis of recent leo satellite constellations: Capabilities and innovative trends," in *2025 IEEE Aerospace Conference*. IEEE, 3/1/2025 - 3/8/2025, pp. 1–12.

[9] Micro-Epsilon, "Fsm3000," accessed: 04.11.2025. [Online]. Available: https://www.micro-epsilon.de/oem/fast-steering-mirrors/

[10] R. Rüddenklau, S. Barone, E. Garbagnati, S. Spier, and G. Schitter, "Feed-forward compensation of body-pointing uncertainties for laser communication terminals," 2026, [in press].
[11] R. Rüddenklau, F. Rein, C. Roubal, B. Rödiger, and C. Schmidt, "In-orbit demonstration of acquisition and tracking on osiris4cubesat," *Opt. Express*, vol. 32, no. 23, pp. 41 188–41 200, Nov 2024.
[12] S. Dwik, G. Sasikala, and S. Natarajan, "Advancements and applications of position-sensitive detector (psd): a review," *Optoelectronics Letters*, vol. 20, no. 6, pp. 330–338, 2024.
[13] R. Kingsbury, J. Twichell, and S. Palo, "Cobalt optical crosslink terminal," in *Free-Space Laser Communications XXXIV*, ser. Proceedings of SPIE, H. Hemmati and B. S. Robinson, Eds. Bellingham, Washington, USA: SPIE, 2022, p. 31. [Online]. Available: https://www.spiedigitallibrary.org/conference-proceedings-of-spie/11993/2610501/Cobalt-optical-crosslink-terminal/10.1117/12.2610501.full
[14] C. Fuchs, C. Schmidt, B. Rödiger, A. Shrestha, M. Brechtelsbauer, J. R. Molina, J. Pacheco, and V. Gstaiger, "DLR's free space experimental laser terminal for optical aircraft downlinks," in *Free-Space Laser Communication and Atmospheric Propagation XXIX*, H. Hemmati and D. M. Boroson, Eds., vol. 10096, International Society for Optics and Photonics. SPIE, 2017, p. 1009610. [Online]. Available: https://doi.org/10.1117/12.2254791
[15] R. Rüddenklau, H. Zeihsel, F. Rein, S. Spier, and J. R. Nonay, "Master attitude controller for modular laser communication systems," *IFAC-PapersOnLine*, vol. 59, no. 31, pp. 73–78, 2025, 1st IFAC Workshop on Control Aspects of Multi-Satellite Systems CAMSAT 2025.
[16] R. Rüddenklau and G. Schitter, "Optimization of acquisition patterns for establishing inter cubesat optical communications," *J. Opt. Commun. Netw.*, vol. 16, no. 8, pp. 814–821, Aug 2024.
[17] M. Goy, J. Krause, O. Bayraktar, P. Ancsin, F. David, T. Dirmeier, N. Doell, J. Dwan, F. Fohlmeister, R. Freund, T. A. Goebel, J. Hilt, K. Jaksch, O. Kohout, T. Kopf, A. Krzic, M. Leipe, G. Leuchs, C. Marquardt, K. L. Mendez, A. Milde, S. Mishra, F. Moll, K. Paciorek, N. Pavlovic Tucakovic, S. Richter, M. Rothe, R. Rüddenklau, G. Sauer, M. Schell, J. Schreck, A. Schreier, S. Sharma, S. Spier, C. Spiess, F. Steinlechner, A. Tünnermann, H. Vural, N. Walenta, and S. Weide, "Ad-hoc hybrid-heterogeneous metropolitan-range quantum key distribution network," *New Journal of Physics*, vol. 27, no. 11, p. 114510, nov 2025. [Online]. Available: https://doi.org/10.1088/1367-2630/ae1864
[18] E. Garbagnati, R. Rüddenklau, and C. Schmidt, "Augmenting attitude knowledge for optical communication terminals on cubesats by kalman filter based estimation." [Online]. Available: https://doi.org/10.26077/c6b4-1384